GeoHealth

RESEARCH ARTICLE

10.1029/2023GH000938

Key Points:

- A new satellite-based emissions inventory for oil and gas flaring and venting is developed to refine existing U.S. emissions inventories
- 710 premature deaths dominate the \$7.3B monetized values of health impacts due to this sector
- Significant benefits in air quality and health could be gained by reducing emissions from flaring and venting activities

Supporting Information:

Supporting Information may be found in the online version of this article.

Correspondence to:

S. Arunachalam,
sarav@email.unc.edu

Citation:

Tran, H., Polka, E., Buonocore, J. J., Roy, A., Trask, B., Hull, H., & Arunachalam, S. (2024). Air quality and health impacts of onshore oil and gas flaring and venting activities estimated using refined satellite-based emissions. *GeoHealth*, *8*, e2023GH000938. https://doi.org/10.1029/2023GH000938

Received 5 SEP 2023
Accepted 31 JAN 2024

Air Quality and Health Impacts of Onshore Oil and Gas Flaring and Venting Activities Estimated Using Refined Satellite-Based Emissions

Huy Tran[1], Erin Polka[2], Jonathan J. Buonocore[2], Ananya Roy[3], Beth Trask[3], Hillary Hull[3], and Saravanan Arunachalam[1]

[1]Institute for the Environment, The University of North Carolina at Chapel Hill, Chapel Hill, NC, USA, [2]Department of Environmental Health, Boston University School of Public Health, Boston, MA, USA, [3]Environmental Defense Fund, Washington, DC, USA

Abstract Emissions from flaring and venting (FV) in oil and gas (O&G) production are difficult to quantify due to their intermittent activities and lack of adequate monitoring and reporting. Given their potentially significant contribution to total emissions from the O&G sector in the United States, we estimate emissions from FV using Visible Infrared Imaging Radiometer Suite satellite observations and state/local reported data on flared gas volume. These refined estimates are higher than those reported in the National Emission Inventory: by up to 15 times for fine particulate matter ($PM_{2.5}$), two times for sulfur dioxides, and 22% higher for nitrogen oxides (NO_x). Annual average contributions of FV to ozone (O_3), NO_2, and $PM_{2.5}$ in the conterminous U.S. (CONUS) are less than 0.15%, but significant contributions of up to 60% are found in O&G fields with FV. FV contributions are higher in winter than in summer months for O_3 and $PM_{2.5}$; an inverse behavior is found for NO_2. Nitrate aerosol contributions to $PM_{2.5}$ are highest in the Denver basin whereas in the Permian and Bakken basins, sulfate and elemental carbon aerosols are the major contributors. Over four simulated months in 2016 for the entire CONUS, FV contributes 210 additional instances of exceedances to the daily maximum 8-hr average O_3 and has negligible contributions to exceedance of NO_2 and $PM_{2.5}$, given the current form of the national ambient air quality standards. FV emissions are found to cause over \$7.4 billion in health damages, 710 premature deaths, and 73,000 asthma exacerbations among children annually.

Plain Language Summary Pollutant emissions from onshore flaring and venting activities in the oil and gas sector are often hard to capture, creating inaccuracies in estimates of air pollution and health impacts from this sector. Here we use remote sensing and reported activity to create a refined estimate of emissions which reveal significant underestimates in official emissions estimates. These emissions contribute to air pollution, which results in \$7.4 billion in health damages annually due to hospitalizations, emergency room visits, worsening asthma, and premature death among downwind populations.

1. Introduction

Flaring is an oil and gas (O&G) industry term used to describe the practice of burning off excess natural gas that is produced along with crude oil, often called "associated gas" or "associated petroleum gas." This associated gas is a valuable commodity when it can be appropriately separated from oil and transported. In practice, however, a facility to support such processing is often absent, and thus flaring is used as a way to dispose of unwanted gas that would otherwise pose a safety hazard or interfere with oil production (DOE, 2019; GGFR, 2023). Multiple economic and technical reasons for why flaring of associated gas is needed are discussed by Soltanieh et al. (2016). According to the World Bank's Global Gas Flaring Reduction Partnership (GGFR, 2023), global gas flaring stayed relatively constant throughout 2010 to 2020 and reached 150 billion cubic meters (BCM) in 2020, equivalent to the total annual gas consumption of sub-Saharan Africa, with the top five flaring countries being Russia (24 BCM), Iraq (17 BCM), Iran (13 BCM), U.S. (12 BCM), and Algeria (9 BCM). Venting of associated gas from O&G compression, processing equipment due to system upset conditions, or pressure release during emergency is also common in O&G production and processing (DOE, 2019).

Besides emitting carbon dioxide (CO_2), O&G flaring releases various pollutants including methane (CH_4), black carbon (soot), nitrogen oxides (NO_x), sulfur dioxide (SO_2), carbon monoxide (CO), and various volatile organic compounds (VOCs) depending on flaring conditions and composition of the associated gas (Anejionu et al., 2015;

Fawole et al., 2016; Umukoro & Ismail, 2017), all of which can cause various impacts on climate, air quality, and human health. According to the World Bank's Global Gas Flaring Tracker Report, flaring released over 400 million tons of carbon dioxide equivalent (CO_2e) emissions into the atmosphere in 2020 (World Bank, 2022); such amount is roughly equivalent to the greenhouse gas emissions of around 77 million cars. Allen et al. (2016) estimated that in the U.S., O&G flaring contributes 20 to 21 million metric tons of CO_2e of greenhouse gases per year. Evaluating O&G flaring's impact on nationally determined contributions (NDC) defined under the United Nations Framework Convention on Climate Change Paris Agreement, Elvidge et al. (2018) found global flaring represents less than 2% of the NDC reduction target; however, some countries (e.g., Yemen, Algeria, Iraq) may fully meet their NDC reduction target by just controlling for flaring.

Cushing et al. (2021) estimate more than 500,000 Americans living within 3 miles of natural gas flares and are at risk of adverse health effects. O&G production in the U.S. has adverse health impacts of 7,500 premature deaths and 410,000 asthma exacerbations annually (Buonocore et al., 2023). Emissions from flaring cause an increase in respiratory diseases, heart diseases, and strokes due to black carbon particle exposure (Chen et al., 2022). Studies report an observed association between flaring activity and increased risk of preterm birth in the Eagle Ford Shale (Cushing et al., 2020) and respiratory hospital visits in North Dakota (Blundell & Kokoza, 2022). Motte et al. (2021) evaluated flaring's impacts on human health due to both local emissions of air pollutants and its contribution to climate change and found that globally, flaring contributed about 0.12% of the health impacts related to $PM_{2.5}$, and 6.51% of the health impacts related to climate change.

Operators of O&G production facilities which perform flaring and venting (FV) report the volume to local regulatory agencies. However, indicators show that the flared and vented volume reported through this mechanism is underreported (BBC, 2022; DOE, 2019). Methane emissions from O&G flaring in the U.S. have been found to be more than five times higher than what was expected (Plant et al., 2022). In New Mexico, North Dakota, and Texas, the flared gas volume estimated from satellite observation is as much as double the volume reported to the states during the years 2012–2017 (DOE, 2019). In 2019, about 15.2 BCM of total vented and flared gas was reported over the U.S. (EIA, 2023) while flared gas alone is estimated at 17.3 BCM from satellite observations (EOG, 2023). Willyard and Schade (2019) found that self-reporting flared gas volume was about half of what was estimated from satellite observations taken from 2012 to 2015. Thus, the use of self-reported gas volumes exclusively could lead to an underestimation of emissions from flaring and venting.

Although the destruction efficiency (i.e., percent of hydrocarbon compounds in flared gas that are converted to carbon dioxide) of flaring is often assumed to be greater than 95% (Caulton et al., 2014; Gvakharia et al., 2017; Pohl et al., 1986; Shaw et al., 2022), incomplete combustion and unlit flares are not uncommon and these issues can lead to lower destruction efficiency of flaring (Lyon et al., 2021; Plant et al., 2022; Tyner & Johnson, 2021).

Discrepancies in emission estimates from O&G in the National Emission Inventories (NEI) have been discussed in previous studies (e.g., Francoeur et al., 2021; Gorchov Negron et al., 2018). Gorchov Negron et al. (2018) compared the NO_X emissions from O&G production estimated by the Fuel-based Oil and Gas inventory (FOG) to the NEI 2017 and found that the NEI overestimates NO_X by over a factor of two in three out of four studied basins. Francoeur et al. (2021) showed that NO_X and VOC emissions from O&G in 2015 were about 40% lower and up to two times higher, respectively, in FOG than in the NEI 2014.

In this study, we address the potential underestimation of flaring and venting emissions in the current National Emission Inventory (NEI), by using flared gas volume estimates from the Visible Infrared Imaging Radiometer Suite (VIIRS) and other industry emission inventories. Estimating emissions from O&G flaring using VIIRS observations has been performed in earlier studies (Chen et al., 2022; Dix et al., 2019, 2022; Francoeur et al., 2021; Zhang et al., 2015). We further investigate the impacts of flaring and venting from O&G production and processing in the U.S. on air quality and human health related to both gas-phase and aerosol pollutants using an integrated assessment framework previously used to evaluate health impacts of oil and gas production in the U. S. (Buonocore et al., 2023).

2. Materials and Methods

2.1. Flare Emissions From NEI

In the NEI 2017, a small fraction of emissions from flaring are classified as O&G point sources; most of the flaring emissions are not separated out but rather lumped into total emissions of O&G nonpoint sources, and hence reported at a county resolution. We identified 22 source classification codes (SCC) of O&G point sources from the NEI 2017 that have the "flare" keyword in the descriptions of SCC (Table S1 in Supporting Information S1). Some of these 22 SCCs have zero emissions, and most emissions are from the top four SCCs (reported in Table S1 in Supporting Information S1). Among O&G nonpoint sources in the NEI 2017, six SCCs represented flaring from well completions and only two SCC reported non-zero emissions. Personal communications with technical staff in charge of O&G emissions inventory development in EPA Office of Air Quality Planning and Standard, Texas Commission on Environmental Quality (TCEQ) (TCEQ, 2004) , Colorado Department of Public Health and Environment, Wyoming Department of Environmental Quality, and Utah Department of Environmental Quality (UDEQ), identified 19 nonpoint SCCs associated with flare emissions (as shown in Tables S2 and S3 in Supporting Information S1), and many of these do not have the keyword "flare" in the SCC descriptions.

Not all O&G equipment (e.g., condensate tanks, crude oil tanks) represented by these 19 SCCs are equipped with flares. Therefore, flare emissions from the 19 nonpoint SCCs vary among U.S. counties—the spatial resolution at which the nonpoint O&G emissions are allocated in the NEI. To estimate NEI 2017-derived flare emissions for each county in the CONUS, we first applied records with non-zero NO_X emissions as an indicator for with-flare emissions from each of the 19 nonpoint flare-SCCs, then emissions of all criteria pollutant from the same SCC are classified as from flaring.

Due to the high destruction efficiency of flares (>95%), VOC emissions from flare stack mounts, while containing highly reactive precursors for ozone and hazardous air pollutants (e.g., Knighton et al., 2012; Olaguer, 2012a), are assumed be close to zero. However, flares are not always operating properly which can lead to increased venting of natural gas through the flare stack flaring (DOE, 2019; Lyon et al., 2021; Plant et al., 2022; Reuters, 2022; Tyner & Johnson, 2021). For example, Lyon et al. (2021) reported that 11% of surveyed flares in the Permian Basin had combustion issues and 5% were unlit and emitted uncombusted gas directly into the atmosphere. In the NEI, we were unable to distinguish between improper flaring and venting VOC. Based on our personal communication with TCEQ staff, we learned that VOC emissions from minor with-flare sources (e.g., condensate and crude oil tanks with non-zero NO_X emission) are the combination of VOC emissions from vented gas (major) and the remaining from flaring (minor). We assumed that, if routine flaring of associated gas was to be eliminated and the would-be flared gas be captured instead through other means of emission controls, it is reasonable to have some sources of vented gas at the same facility be captured in the same way. It is also reasonable to assume regulatory drivers limiting or prohibiting routine flaring of associated gas would result in corresponding reductions in routine venting of associated gas. Therefore, in this study, we considered VOC emissions from the 19 nonpoint flare-SCCs as from venting and combined this VOC emissions estimate with non-VOC emissions from flare into the same group of "flaring and venting" (FV). Note that "venting" in this way only represents VOC emissions from vented gas from O&G sources equipped with a flare using the non-zero NO_X emissions criteria as discussed above. We assume this approach captures all possible VOC emissions from O&G sources associated with flare.

Figure 2 shows emissions of criteria pollutants from O&G categories including point- and nonpoint-flares, as derived from NEI 2017. FV is also found to account for 10% of the total 7.3 million tons per year of methane from O&G, although this is not a targeted pollutant for discussion on air quality and health impacts in this study.

2.2. Flare Emissions Estimation From VIIRS

The VIIRS Nightfire data set (Elvidge et al., 2013; Elvidge et al., 2015; EOG, 2023; Zhizhin et al., 2021) was processed for annual natural gas flared volume in the U.S. from 2017 to 2020 (Figure 1). In 2019, the year with highest flare gas volume during the above period, there were 17.7 BCM of natural gas flared in both production (97%) and processing (3%)—the same amount of flare gas volume was reported in Chen et al. (2022). We performed the following processing on VIIRS data prior to emissions estimation: only onshore flares were considered; VIIRS-detected flares are excluded if they were found to be in proximity of NEI 2017 point flare sources to avoid double counting. As a result, there were 17.3 BCM of VIIRS-detected flared gas remaining for emissions estimation. We applied the gas heating values and emission factors derived from previous studies and from our personal communications with emission inventory developers in Texas, New Mexico, Colorado, Wyoming, and Utah. In comparison to NEI, several improvements were made to estimations of flare emissions where we treated VIIRS-detected flares as point sources, estimated directly emitted primary particulate matter (in

10.1029/2023GH000938

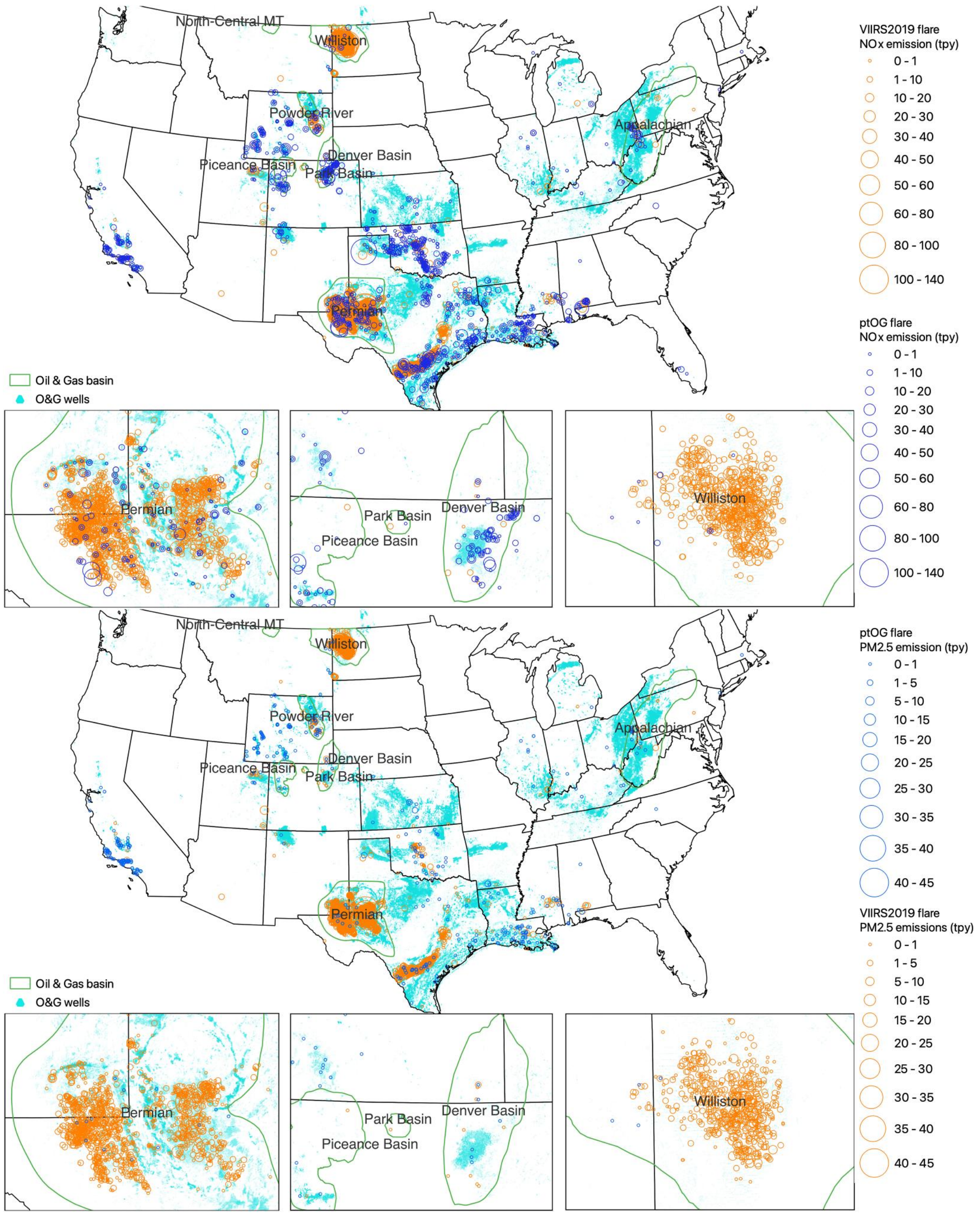

Figure 1. Combined NO_X (top) and $PM_{2.5}$ (bottom) emissions from FV as estimated from VIIRS and as derived from NEI 2017 point O&G (ptOG flare).

form of black carbon) and SO_2 emissions, utilized empirical algorithms for flare stack parameters, and employed state-level monthly flared and venting gas volume for temporal allocations. Additional methodologic details are described in Text S2 in Supporting Information S1.

There is a high probability that not all flares were adequately detected by VIIRS. Certain criteria must be met for a flare to be detected by VIIRS, such as flared temperature >1,400 K, frequent combustion (consistency), and free of cloud cover and other contaminations (C. Elvidge et al., 2013, 2015). In our case study for the Uinta O&G basin in Utah, we compared the number of VIIRS-detected flares with the self-reported flare data from O&G operators (UDEQ, 2022) and found that only 11 reported flares (or 8%) of the 132 reported flares were detected by VIIRS in 2019.

Table 1
Annual Emissions (tpy) of Criteria Pollutants From Flaring and Venting (FV)

	$PM_{2.5}$	NH_3	VOC	CO	NO_X	SO_2
NEI 2017 point flare	7.82E + 01	1.84E − 01	4.59E + 03	8.44E + 03	2.71E + 03	1.53E + 04
NEI 2017 nonpoint flare	2.22E + 02	0	1.31E + 06	3.94E + 04	1.87E + 04	3.37E + 04
Total NEI 2017 flare	3.00E + 02	1.84E − 01	1.31E + 06	4.78E + 04	2.14E + 04	4.90E + 04
VIIRS-only flare[a]	4.34E + 03 ±178	0	1.04E + 06	6.79E + 04 ±744	1.42E + 04 ±237	8.98E + 04 ±3,659
VIIRS + Rystad + NEI hybrid	4.82E + 03	0	1.31E + 06	7.75E + 04	2.33E + 04	1.00E + 05
Total *wFlare1*[b]	4.42E + 03 (1,373%)	1.84E − 01 (0%)	1.04E + 06 (−20%)	7.63E + 04 (60%)	1.69E + 04 (−21%)	1.05E + 05 (114%)
Total *wFlare2*[b]	4.90E + 03 (1,533%)	1.84E − 01 (0%)	1.31E + 06 (0%)	8.59E + 04 (80%)	2.60E + 04 (22%)	1.15E + 05 (135%)

[a]See Supporting Information S1 for method of estimating emission uncertainties. [b]Numbers in parentheses indicate changes in emissions from NEI 2017: for example, 100*(*wFlare2* − NEI 2017)/NEI 2017.

Another uncertainty in VIIRS flare data is the flare gas volume (FGV). VIIRS estimates FGV by applying regression algorithms to the relationship between radiated heat energy from detected flare to the reported FGV at country and state-level resolution (C. Elvidge et al., 2013, 2015). Uncertainties of the regression algorithms are estimated to be ±9.5% (Elvidge et al., 2015). Another source of uncertainty is from the country- and state-level reported FGVs, which are subject to known and unknown biases as discussed by Schade (2021). Large gaps exist when VIIRS-estimated FGV in 2019 is compared to FGV reported by Rystad Energy (2022) for the same year (Table S4 in Supporting Information S1). For example, Rystad Energy (2022) reports FGV in Colorado in 2019 to be 136 MCF/yr, whereas only 18 MCF/yr is estimated by VIIRS. Non-detection of flares by VIIRS (more discussion on this later) in Colorado is partially attributed to this gap. Since no uncertainty was reported for VIIRS's FGV in 2019 as well as in other years, this type of uncertainty was not incorporated in estimation of FV emissions in this study.

To account for the potential under-estimation of FGV and, consequently, the under-estimation of emissions from FV, we developed two emissions scenarios for FV. The *wFlare1* scenario estimates emissions of criteria pollutants solely based on VIIRS-estimated FGV and existing point O&G flares in the NEI. In *wFlare1* scenario, we replaced the NEI 2017 emission estimates of NO_X, CO, SO_2, and $PM_{2.5}$ from the 19 nonpoint SCCs (discussed above) with corresponding estimates based on VIIRS-detected flares; we incorporated the NEI 2017 emission estimates of the 22 O&G flare point sources (discussed above) as-is. The *wFlare2* combines emissions in *wFlare1* with additional emissions estimated for FGV reported by Rystad Energy (2022) and FV emissions derived from NEI 2017. Specifically: in each county where either VIIRS's, Rystad's, or NEI 2017s estimates exist, VIIRS's estimates are first compared against Rystad's. If Rystad's estimates are larger than VIIRS's, differences between the two are added to VIIRS's. If Rystad's estimates are not available or lower than VIIRS's, VIIRS's estimates are then compared against NEI 2017s. Differences between the two estimates are added to VIIRS's if NEI 2017s estimates are higher. In this sense, *wFlare2* represents a hybridized estimate of FV which partially compensates for missing FV data in any one source.

Due to our approach to treatment of VOC emissions from FV, total VOC emissions from O&G based on NEI 2017 are identical in *wFlare1* and *wFlare2*. VOC emissions from O&G attributed to nonpoint FV in *wFlare2* are based on NEI 2017, but higher than the emissions in *wFlare1* (Table 1).

2.3. CMAQ Model Configurations and Model Performance Evaluation

The model configurations in this study refined the configurations applied in Buonocore et al. (2023), which evaluates impacts of O&G emissions to air quality and public health in 2016. As such, all anthropogenic and wildfire emissions other than O&G are based on the NEI 2016 v1. Emissions from all other O&G sources other than FV are taken from the NEI 2017. The use of NEI 2017 instead of NEI 2016 v1 for O&G sources are due to two factors: introduction of new flare-SCCs as discussed above; and NEI 2017 is the latest national baseline estimate from the EPA and furthermore, it better represents year 2019 in which FGV is highest and for which FV emissions are estimated for.

The Models-3/Community Multiscale Air Quality (CMAQ) modeling system (Byun & Schere, 2006; Wyat Appel et al., 2018) version 5.2.1 was utilized to simulate atmospheric chemistry with Carbon-Bond version 6 revision 3 (CB6r3) gaseous chemistry and aero6 for aerosol treatment. Meteorological inputs are derived from the Weather Research and Forecasting model (Skamarock et al., 2008) version 4.7. WRF-CMAQ simulations were performed for January, April, July, and October 2016 (to represent four seasons) for a modeling domain covering the conterminous U.S. (CONUS) in 12 km × 12 km horizontal grid resolution and 35 vertical layers (12US1 domain). Boundary and initial chemistry conditions were taken from the hemispheric CMAQ (HCMAQ) version 5.2.1 simulation for the northern hemisphere. Evaluation of CMAQ model performance for key pollutants of interest are briefly discussed in Text S3 in Supporting Information S1.

Two model scenarios included FV emissions as estimated in *wFlare1* and *wFlare2* (discussed above) and all other non-FV emissions from all other anthropogenic and natural sources in the domain. FV emissions are excluded in a zero-out scenario (*woFlare*). Simulation results of *wFlare1* and *wFlare2* are compared against *woFlare*, alternatively, to quantify the impact of FV emissions on air quality and human health. For brevity, however, discussions on the impacts in the following sections are based on *wFlare2* scenario unless specified otherwise.

2.4. Analyses

Modeled exceedance counts are determined for each of *woFlare* and *wFlare2* scenarios and then differences were used to determine marginal impact of flaring and venting emissions on the National Ambient Air Quality Standard (NAAQS) threshold(s). A modeled exceedance event is identified when concentration in any grid-cell for any pollutant exceeded its corresponding NAAQS for the relevant timescale: for example, Maximum Daily 8-hr average Ozone (MDA8O3) at any grid-cell for any day exceeded 70 ppb. For this study, the model domain is 459 (columns) × 299 (rows) grid-cells and there are 123 simulation days in total. Thus, there are up to 459 × 299 × 123 possibilities for MDA8O3 or Daily Average $PM_{2.5}$ exceedances to occur. Note that a high number of exceedances does not necessarily lead to violation of NAAQS.

2.5. Method for Health Impact Analyses

To estimate the health impacts of ambient ground level concentrations of $PM_{2.5}$, NO_2, and ozone, we used BenMAPR, which is a geospatial health impact assessment model in R that is based on the Benefits Mapping and Analysis Program (BenMAP) from the U.S. EPA (Sacks et al., 2018), and was used in two recent studies (Arter et al., 2022; Buonocore et al., 2023). BenMAPR accepts gridded air pollution concentration outputs from CMAQ and overlays them with (a) population data from the U.S. American Community Survey from the U.S. Census Bureau; (b) data on background rates of health outcomes from the U.S. Centers for Disease Control, Health Care Utilization Project, and BenMAP from the U.S. EPA; and (c) concentration response functions relating air pollution exposure and changes in risks for health outcomes from the epidemiological literature. To calculate the health impacts of flaring, we subtracted the health impacts of air pollution under the Baseline/No-flaring scenario from those of the *wFlare2* scenario to isolate the health impacts from the flare portion of *wFlare2* scenario emissions. The estimated flaring air pollution attributable health outcomes were then monetized using valuation methods from the U.S. EPA and existing health literature. Details of the background health data sets, concentration response functions, and valuation functions are available in Tables S9 through S11 in Supporting Information S1. Methods for additional health impact analyses, including environmental justice, are presented in Text S2 in Supporting Information S1.

3. Results and Discussion

3.1. Flare and Venting Emissions

The inclusion of $PM_{2.5}$ and SO_2 to FV emissions resulted in significantly higher emissions of the two pollutants in both *wFlare1* and *wFlare2* than in NEI 2017 over the entire CONUS (Table 1, Figures S2 and S3 in Supporting Information S1). Compared to NEI 2017, FV $PM_{2.5}$ emissions are 13 times and 15 times higher in *wFlare1* and *wFlare2*, respectively. FV SO_2 emissions are more than two times higher in *wFlare1* and *wFlare2* than in NEI 2017. As discussed in Text S2 in Supporting Information S1, O&G SO_2 emissions are highly underestimated in the NEI 2017 and our FV SO_2 emissions are likely closer to actual emissions. Since VIIRS did not detect flares in some counties where FV emissions were reported in NEI 2017, VOC, and NO_X emissions are lower in *wFlare1* than in NEI 2017. In *wFlare2* where excess emissions from Rystad and NEI 2017s estimates are considered, FV

10.1029/2023GH000938

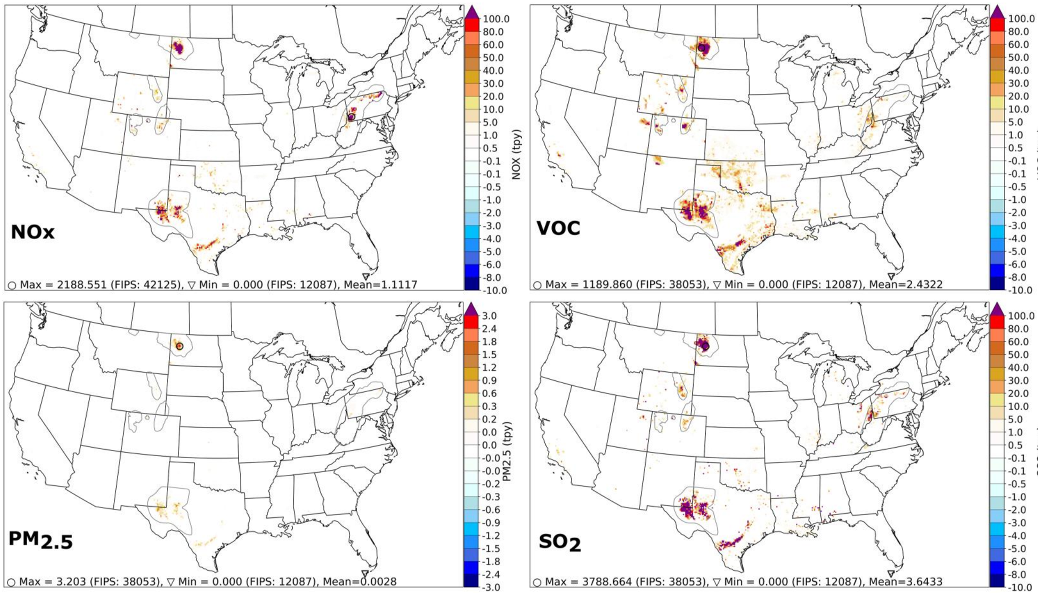

Figure 2. Annual emissions (tpy) of NO_X, VOC, $PM_{2.5}$, and SO_2 from flaring and venting (FV).

NOx emissions are 22% higher than NEI 2017 and VOC emissions match the NEI 2017s estimates. NH_3 emissions are identical among all three estimates as NH_3 emissions are only accounted as point flares in the NEI 2017 and no NH_3 emissions were accounted for in the VIIRS-detected flares.

Large gaps exist between VIIRS-detected and NEI-derived flares. Figure 1 shows NO_X and $PM_{2.5}$ emissions as estimated using VIIRS flared gas volume (FGV) and as derived from point O&G flare categories from NEI 2017. Most VIIRS-detected flares are over O&G production fields, including Permian in New Mexico (NM) and Texas (TX), Eagle Ford in TX, and Bakken/Williston in North Dakota (ND); whereas a lot fewer VIIRS-detected flares exist over other major O&G production fields such as the Barnett, Denver basin or Appalachian in Pennsylvania (PA) (Figure 1). On the one hand, the NEI-derived flares are reported in more O&G production fields. Over the Denver basin in Colorado (CO), for example, most flares are from NEI-derived data and not detected by VIIRS. On the contrary, over the Bakken basin, the largest flare FVs are VIIRS-detected and very few are from NEI-derived data.

In accordance with the distribution of VIIRS-detected flares, emissions from FV are most noticeable in major O&G production fields in the U.S., especially those in NM, TX, ND, CO, and WY (Figure 2). Emissions differences between *wFlare2* and *wFlare1* (i.e., FV emissions accounted for in the NEI 2017 but not in VIIRS) are shown in these states but also noticeable in Oklahoma, Kansas, Pennsylvania, Ohio, and West Virginia (Figures S5 and S6 in Supporting Information S1). In Pennsylvania (Appalachian basin), between *wFlare2* and *wFlare1* there is a distinctly high FV NOx emissions hotspot which comes from a single flare-SCC (2310021500) for flaring from an onshore gas well completion. This distinctly high NO_X emission is attributed as an artifact in NEI 2017 and is treated "as is" in this study. As $PM_{2.5}$ emissions were only estimated for VIIRS-detected flares, there are no $PM_{2.5}$ emissions differences between *wFlare2* and *wFlare1*. $PM_{2.5}$ emissions from FV account for about 82% of total O&G $PM_{2.5}$ emissions (Table S6 in Supporting Information S1). In this study, FV SO_2 emissions account for 82% of total O&G SO_2 emissions, and this high percentage is attributed to underestimation of O&G SO_2 emissions in the NEI 2017 (see Text S2 in Supporting Information S1). VOC emissions from FV account for about 50% of total O&G VOC emissions over the CONUS mainly due to the inclusion of storage tank's venting. The benefit of treating FV VOC emissions in this study, however, provides an opportunity to quantify air quality and health benefits from potentially controlling both flaring and venting together.

This study estimates black carbon (BC) (analogous to primary $PM_{2.5}$) emissions in the CONUS from FV to be 4,340 ± 178 tpy with Texas (2,244 ± 129 tpy) and North Dakota (1,713 ± 111 tpy) as the top two emitting states. Chen et al. (2022) estimated BC emissions from upstream flaring in the CONUS to be 15,986 tpy, with ND (10,036 tpy) and TX (4,317) as the two leading states. A different set of emission factors and heating values

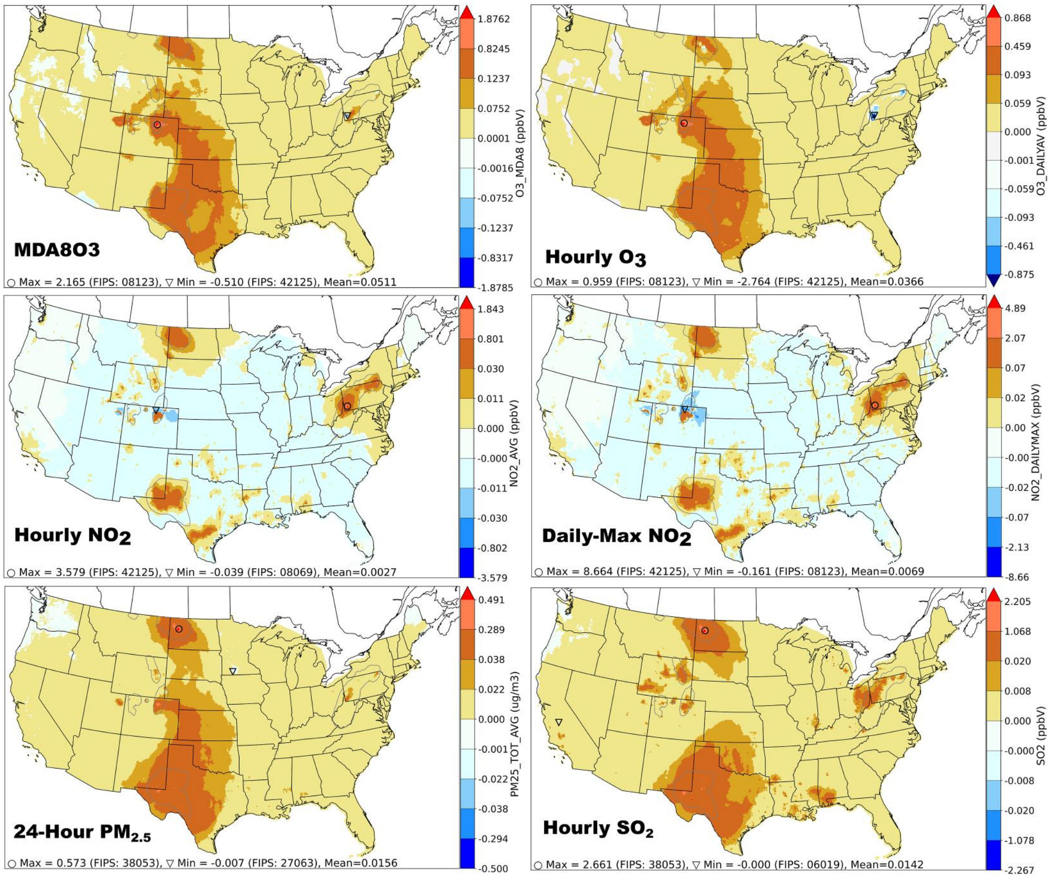

Figure 3. Annual-average of MDA8 Ozone (ppb), 24-hr average $PM_{2.5}$ ($\mu g/m^3$), daily-average and daily-maximum NO_2 (ppb), SO_2 (ppb) contributed by FV (i.e., differences between *wFlare2* and *woFlare*).

applied in Chen et al. (2022) gives reason for their higher estimations of $PM_{2.5}$ emissions than in this study. Although the VIIRS-detected flare gas volume is higher in TX (8.73 BCM) than in ND (6.09 BCM), Chen et al. (2022) estimated higher BC in ND because of the higher heating value applied to this region. Based on in-situ measurements in 2013–2014, Schwarz et al. (2015) estimate BC emissions in the Bakken basin to be 1,400 ± 360 tpy, which is relatively closer to our estimates. Only about 0.36 Gg per year (or 397 tpy) of BC emissions from flaring in the Bakken basin were estimated by Weyant et al. (2016).

Dix et al. (2019) estimated NO_X emissions from VIIRS-detected flaring in 2018 in the Permian and Bakken basins to be 12.6 ± 0.6 and 11 ± 0.6 tons per day (equivalent to 4,599 ± 219 tpy and 4,015 ± 219 tpy), respectively. Using the same VIIRS-detected flare approach, Francoeur et al. (2021) estimated NO_X emissions from flaring in 2015 to be 3,650 ± 2,847 tpy in Permian, 2,628 ± 1,752 tpy in Bakken, 21.9 ± 14.6 tpy in Denver-Julesburg and 14.6 ± 11 tpy in the Marcellus (Appalachian). Our estimates of NOx emissions from VIIRS-detected flares in 2019 are 6,925 ± 169 tpy in Permian, 5,355 ± 149 tpy in Bakken, 82 ± 8 tpy in Denver-Julesburg, and 33 ± 7 tpy in Appalachian, and given that VIIRS-detected flared gas volume in 2019 is the highest in recent years (Table S4 in Supporting Information S1) (Note that it is unclear how emission uncertainties were determined for each O&G basin in Francoeur et al. (2021) and Dix et al. (2019)).

3.2. Impact of Flaring and Venting on Air Quality

Domain-wide annual average impacts of FV on O_3, NO_2, and $PM_{2.5}$ concentrations in the CONUS are relatively small (<0.15%). However, the impacts greatly vary with locations and seasons (Figure S7 through S12 in Supporting Information S1), with the strongest impacts typically occurring in areas with intense FV emissions (Figure 3), emphasizing the advantage of the detailed treatment of the emissions and processes at the modeled grid resolution of 12 km × 12 km over the entire country.

3.2.1. Impacts on MDA8O3

FV's impact on O_3 is stronger in January than in other months (Figure S9 in Supporting Information S1). FV is found to contribute 4%–47% (4–16 ppb) and 2%–15% (2–10 ppb) of MDA8O_3 in January and July, respectively, over FV-major areas (e.g., Permian, Denver, Bakken). Among O&G production fields with emissions from FV (referred hereafter as FV-major areas), the Denver basin observed the highest FV impact on MDA8O_3 (up to 16 ppb or 47%, occurred in January indicating FV contribution to wintertime ozone) followed by Bakken (10 ppb, 19%, July) and Permian (7 ppb, 11%, October) as the second and third highest impacted basins. The impact on MDA8O_3 is also noticeable in areas within 100 km of FV-major areas (4–6 ppb or 9%–30%) but reduces to less than 1 ppb (5%) elsewhere. We found high NO_X emissions in the Appalachian basin enhanced O_3 formation for the area in July (up to 3 ppb) but suppressed O_3 formation by as much as −3.5 ppb in other months (Figure S9 in Supporting Information S1). Differences in FV's impact on O_3 between *wFlare2* and *wFlare1* scenarios (Figure S8 in Supporting Information S1) closely follow the differences in NO_X and VOC emissions between the two scenarios (Figure S6 in Supporting Information S1) and is less than 2 ppb for impacts on MDA8O_3.

Note that the CMAQ domain used in this study at a 12 km × 12 km horizontal resolution could cause potential biases in the estimated ozone impacts from FV. Flares are small point sources, which create plumes of reactive hydrocarbons and NO_X that are subgrid-scale. Due to non-linear ozone formation with NOx, the formation of ozone inside these plumes will proceed differently than in the grid-based model treatment, where emissions are instantaneously diluted into the much larger model grid-cell as compared to narrow emissions plumes. Olaguer (2012b, 2012a) showed that degrading the model domain from 200 m to 1 km horizontal resolution could, depending on the emission compositions, either enhance or reduce the estimation of ozone impacts from a flare source.

3.2.2. Impacts on NO_2

FV's impacts on NO_2 are particularly heterogeneous over space and time. FV emission driven increases in NO_2 concentrations are mostly localized to areas with FV emissions, and reduction of NO_2 are observed in some areas, especially downwind of the Denver-Julesburg and Uinta basins (Figure 3, Figure S10 in Supporting Information S1). The response of NO_2 concentration to FV's emissions depends on local background chemistry. During the daytime, NO_2 and NO interconvert through photolysis reactions and through reactions with O_3, organic (ROx) and hydrogen oxide radicals (HOx). NO_X is terminated by forming nitric acid (HNO_3) and dinitrogen pentoxide (N_2O_5, nighttime only), in which both are precursors of nitrate aerosols. Within the immediate proximity of FV sources, NO_X together with VOC-enhanced NO-to-NO_2 conversion due to emissions from FV results in net increase of NO_2 as observed in most FV-major areas. Unlike most other O&G basins where NOx is limited, the Denver-Julesburg (McDuffie et al., 2016) and the Uinta (Ahmadov et al., 2015; Edwards et al., 2013, 2014) basins are known to have background conditions which are NO_X-rich. However, downwind of FV sources in these two basins, the increased NO_X and VOC from FV enhances the HO_X-NO_X cycle quenching effect (as discussed in Womack et al., 2019), which results in reduction of NO_2. NO_2 reductions that occurred elsewhere in the model domain are insignificant (<0.005 ppb) and are attributed to numerical artifacts in the grid resolution used.

Since the partition of nitrate to aerosol is favorable under low temperature conditions (Ansari & Pandis, 1998; Park, 2004), loss of NO_2 through this pathway is higher in January than other months and is lowest in July (Figure S10 in Supporting Information S1). Monthly average hourly NO_2 decreases by 0.1 ppb in January in the downwind areas of Denver and Uinta basins, and parts of these areas observe an increase by 0.5 ppb in monthly average hourly NO_2 in July. The Appalachian basin observes the highest contribution of hourly (up to 8 ppb, or 46% of total NO_2) and daily-maximum (up to 25 ppb, 56%) NO_2, both in July, from FV, followed by the Denver, Permian and Bakken basins where observed contributions in 2–6 ppb (8%–30%) and 2–20 ppb (18%–36%) to hourly and daily-maximum NO_2 are seen, respectively, with highest contributions often seen in January or July. Elsewhere in the CONUS, other than FV-majors and their downwind areas, changes in monthly average of NO_2 are negligible (±0.02ppb, ±0.4%) in both hourly and daily maximum (Figure 3).

3.2.3. Impacts on $PM_{2.5}$

FV's contribution to annual $PM_{2.5}$ is less than 0.01 μg/m^3 (or 0.2% of total $PM_{2.5}$ on average over the CONUS) but is spatially heterogenous. It contributes 0.1 μg/m^3 (3%) over Permian, 0.1 μg/m^3 (4%) over Bakken, 0.01 μg/m^3 (0.2%) over Appalachian, 0.02 μg/m^3 (0.9%) over Powder River, and 0.1 μg/m^3 (1.2%) over Denver basins

(Figure 3). The Denver basin observed the highest FV's contribution by as much as 5 μg/m^3 to daily average $PM_{2.5}$, whereas highest contributions in other FV-major areas are up to 1.5 μg/m^3. Negative $PM_{2.5}$ contributions (reductions due to FV emissions) occurred in Minnesota, Iowa, and other states in the northeast of the CONUS in January, but at a relatively small margin (up to 0.06 μg/m^3 on monthly average). Positive monthly average $PM_{2.5}$ contribution from FV is greatest in January (up to 1.4 μg/m^3, 10%) and lowest in October (0.5 μg/m^3, 16%) (Figure S11 in Supporting Information S1). On average over the CONUS, however, FV's contribution to monthly-average of $PM_{2.5}$ is larger in July (0.018 μg/m^3; 0.5%) than in January (0.012 μg/m^3; 0.3%) due to negative $PM_{2.5}$ contributions (or $PM_{2.5}$ reductions) mostly occurring in January (Figure S12 in Supporting Information S1).

FV's contribution to $PM_{2.5}$ varies with $PM_{2.5}$ compositions which differ significantly among FV-major as well as non-FV areas (Figure S12 in Supporting Information S1). In areas outside FV-major areas, sulfate aerosol (SO_4^-) is the largest component (48%), followed by elemental carbon (EC; 18%), NH_4^+ (15%), organic carbon (OC, 10%) and NO_3^- (4%). In the Bakken basin, the major $PM_{2.5}$ component is EC (61%), followed by NO_3^- (22%), SO_4^- (14%) and less than 3% of other components. A similar distribution is observed in the Permian basin where 50% of $PM_{2.5}$ is EC followed by NO_3^- (29%), SO_4^- (12%), OC (7%) and NH_4^+ (2%). Differing significantly from other FV-major areas, $PM_{2.5}$ in the Denver basin has NO_3^- as a major component (42%), followed by EC (28%), NH_4^+ (13%), OC (12%) and SO_4^- (2%). In relevant to earlier discussions on NO_2 formation in FV-major areas, FV's contributions NO_3^- and NH_4^+ aerosols are largest in Denver basin. Meanwhile, FV's contributions to EC and SO_4^- are largest in Bakken basin. Reductions of NO_3^- and OC aerosol led to reductions of total $PM_{2.5}$ in Minnesota, Iowa, and other states in northeast of the CONUS (Figure S12 in Supporting Information S1). Since there is negligible difference in primary $PM_{2.5}$ emissions from FV between *wFlare2* and *wFlare1*, the differences in $PM_{2.5}$ contributions between the two scenarios (<0.164 μg/m^3 on annual average) are caused by secondary aerosols which are dominated by their inorganic components, that is, NO_3^- and SO_4^- (Figure S8 in Supporting Information S1).

We found $PM_{2.5}$ contributions from FV are mainly driven by its contribution of SO_2 and primary $PM_{2.5}$ (mostly EC) emissions across the CONUS especially in FV-major areas. Whereas in Denver basin and its downwind areas, we found increases in NO_3^- due to FV emissions enhancing the formation of nitric acid which favors the formation of NO_3^-.

3.2.4. Impacts on Exceedance Counts

Overall, FV emissions caused over 210 instances of MDA8O3 exceedances (MDA8O3 > 70 ppb) over four simulated months in 2016. This is about one-third of MDA8O3 exceedances caused by the O&G sector in 2016 reported by Buonocore et al. (2023). In this study, MDA8O3 exceedances are largest in counties of the Denver basin and its downwind area, followed by counties in Permian basin and those in Pennsylvania and Michigan (Table S7 in Supporting Information S1). FV contributes to no MDA8O3 exceedances in January and most of its exceedance contribution occurred only in the summer month of July. Since we modeled only one summer month, we anticipate that the annual count of MDA8O3 exceedances could be even higher for a typical summer season.

Contributions of FV to daily $PM_{2.5}$ exceedances ($PM_{2.5}$ > 35 μg/m^3) are small. While FV added two additional $PM_{2.5}$ exceedances in Pennsylvania and New Jersey, it also reduced two exceedances in Minnesota and New York due to a reduction of $PM_{2.5}$ in these two states in the winter. For comparison, Buonocore et al. (2023) found 29 instances of $PM_{2.5}$ daily exceedances caused by O&G sector in 2016. If $PM_{2.5}$ daily NAAQS were lowered to 30 μg/m^3, FV emissions would contribute 10 instances of exceedances over four simulated months. No additional annual $PM_{2.5}$ exceedances (annual average $PM_{2.5}$ > 12 μg/m^3) were found. FV would have contributed 3 and 1 additional instances of annual exceedances in Pennsylvania and Illinois, respectively, if the annual $PM_{2.5}$ standard were lowered to 10 μg/m^3 (U.S. EPA, 2023a, 2023b).

FV causes no additional NO_2 exceedances (NO_2 > 100 ppb), which is expected given that Buonocore et al. (2023) found no NO_2 exceedances caused by total O&G in 2016. However, if the 1-hr NO_2 standard were lowered to 60 ppb, then it would add 9 instances of exceedances in Colorado and 1 instance in Florida.

Buonocore et al. (2023) estimated that in 2016 the O&G sector contributed 0.6 ppb of O_3, 0.17 ppb of NO_2 and 0.065 μg/m^3 of $PM_{2.5}$ on average over the CONUS. This study found the corresponding contributions from FV are 0.026 ppb, 0.03 ppb and 0.008 μg/m^3, respectively. Since FV emissions do not exist in all areas with O&G activities, such relatively small FV's contribution in comparison to total O&G when taking average over the

CONUS is anticipated. However, the highest FV's contributions to MDA8O3 (15 ppb), daily maximum NO_2 (25 ppb) and daily average $PM_{2.5}$ (5 μg/m^3) are much higher than the values found for total O&G by Buonocore et al. (2023) (3 ppb, 17 ppb, and 1.7 μg/m^3, respectively), emphasizing the near-field impacts of FV that one should focus on. Note that this study combined O&G emissions from NEI 2017 and FV emissions calculated based on VIIRS-Rystad-NEI hybrid data set, whereas Buonocore et al. (2023) utilized O&G emissions from NEI 2016 as is. Regardless, this finding illustrated that estimation of impacts on O&G sectors on air quality, and consequently human health, could greatly vary with input emissions, and improvements in the emissions estimates as we have done provide increased confidence in the modeled estimates.

3.3. Health Impacts of Flaring and Venting

Our results show in 2016, emissions due to flaring in Flare Scenario 2 have a mortality burden of 710 (95% CI: 480–1,100) excess deaths attributable to $PM_{2.5}$, NO_2, and ozone compared to baseline scenario emissions. Additionally, our results show an estimated annual excess of 73,000 (95% CI: 46,000–110,000) childhood asthma exacerbations, 92 (95% CI: 58–140) childhood asthma emergency department visits, and 10 (95% CI: 6.4–15) asthma hospitalizations attributable to $PM_{2.5}$, NO_2, and ozone. An excess of 190 (95% CI: 66–300) childhood asthma incidence and 130 (95% CI: 50–120) respiratory hospitalizations were also found, for combinations of $PM_{2.5}$ and NO_2, and $PM_{2.5}$ and ozone, respectively.

A recent paper (Buonocore et al., 2023) using a similar framework and data inputs showed that the health burden of O&G as a whole is 7,500 (95% CI: 4,500–12,000) deaths, 410,000 (95% CI: 9,200–810,000) childhood asthma exacerbations, and 2,200 (95% CI: 830–3,200) childhood asthma incidences. Comparing these two studies indicates that flaring and venting contributes just under 10% of the mortality cases and incident asthma cases from O&G production, and around 5.4% of the asthma exacerbations from O&G production. FV contributes 2% of NOx emissions, 81% of SO_2, 51% of VOCs, and 18% of $PM_{2.5}$ from O&G. The relative proportions that NO_2 from flaring contributes to total sector deaths and asthma exacerbations (Table S11 in Supporting Information S1) indicate the strong role of NO_2 in driving total health impacts.

Asthma outcomes calculated using all Alhanti CRFs (for NO_2, $PM_{2.5}$, and ozone) are approximately three times larger than those calculated using all the Orellano CRFs (NO_2 and $PM_{2.5}$). The increase in cases is predominantly due to the inclusion of ozone, which accounted for nearly 60% of all Alhanti asthma outcomes. Estimates due to $PM_{2.5}$ and NO_2 were consistently higher for Alhanti than for Orellano. All three asthma related outcomes estimated by Alhanti were three times larger than those estimated by Orellano (Table S11 in Supporting Information S1).

Figure 4 presents spatial distribution of FV air pollution-attributable deaths in 2016. Texas observed the highest FV-attributed premature deaths at 133 incidences, of which 76, 51, and 6 incidences are caused by $PM_{2.5}$, O_3, and NO_2, respectively. The second (115) and third (76) highest premature deaths are observed in Pennsylvania and Colorado, respectively. The top three numbers of FV-attributed asthma incidences by state are also observed in Texas (14,935), Colorado (13,748), and Pennsylvania (11,184). Although being an FV-major area, only 6 premature deaths and 464 asthma incidences were observed in North Dakota, which is explained by the transport of these emissions to downwind locations. Between 20 and 30 FV-attributed premature deaths and 2,000 to 3,000 asthma incidences are observed in Illinois, New York, Ohio, and Oklahoma.

Of the 710 deaths attributable to *wFlare2*, 1 in 3 occurred in low-income census tracts, 1 in 10 occurred in tracts identified as 65th percentile or higher for Native persons (i.e., greater than or equal to 2% Native populations), and 1 in 3 occurred in tracts identified as 65th percentile or higher for Hispanic/Latino-identified persons (i.e., greater than or equal to 14% Hispanic/Latino populations) (Table S12 in Supporting Information S1). Similar proportions of impact were seen for childhood asthma exacerbations among low-income and Native-identified tracts, and a slightly larger proportion of impact was seen among Hispanic/Latino-identified tracts (40%). Low income-identified tracts had 1.1 times the risk of premature mortality from *wFlare2* exposure than tracts not identified as low income (Table S13 in Supporting Information S1). Native-identified tracts had 1.2 times the risk of premature mortality and 1.1 times the risk of childhood asthma exacerbations from *wFlare2* exposure than non-Native-identified tracts. Hispanic/Latino-identified tracts had 1.1 times the risk of childhood asthma exacerbations than non-Hispanic/Latino-identified tracts. Pollutant exposure from *wFlare2* was not found to disproportionately increase the risk of premature death among census tracts identified as Hispanic/Latino, or to disproportionately increase the risk of childhood asthma among low-income tracts.

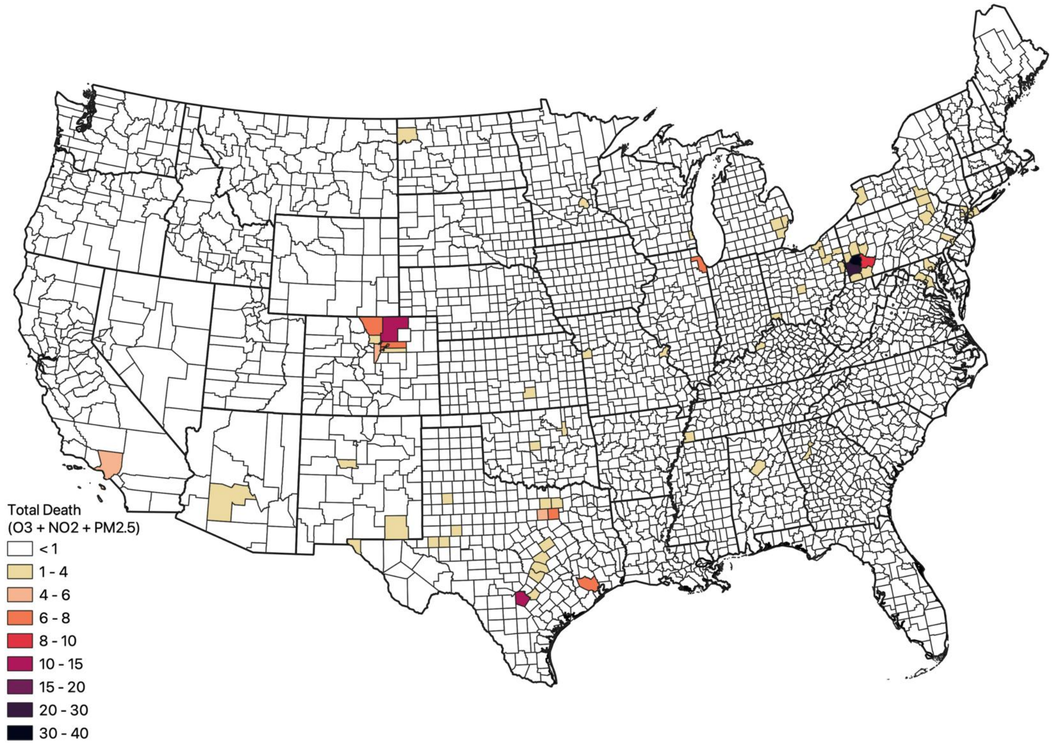

Figure 4. FV air pollution-attributable deaths in 2016.

Table 2 shows that the monetized values of the health impacts due to FV total \$7.4B, while Buonocore et al. (2023) reported \$77B from the entire OG sector, indicating a rather significant (~10%) contribution of FV to the overall monetized health risk from the OG sector. Industry analysis (Rystad Energy, 2022) indicates that solutions for operators to address flaring and capture this otherwise wasted gas are readily available and cost-effective, and even potentially profitable. The results of this study reveal the near-term air quality health benefits from addressing flaring and venting emissions. Since ~90% of the health impacts of O&G production originate from outside flaring, and since NO_2 has such a strong role, this indicates that the health benefits of emission control strategies can be increased by expanding coverage to more NO_X-rich subsectors of the O&G production sector, such as compressors and pumpjack engines, well drilling, and completions, in addition to the solutions for reducing FV emissions.

3.4. Limitations

The analysis year for this study is 2016/2017 based on availability of various input data sets. The flaring volume applied in this study was estimated for 2019, which is the highest estimate from VIIRS throughout the 2017–2022 period (EOG, 2023). So, our flaring emissions estimates in this study could be lower in most recent years. On the other hand, the emissions inventories used here may still be underestimated due to missing flares invisible due to cloud cover and flares too small to detect via satellite. Not all compressor engines are reported in the NEI, and it is possible that other sources are similarly underreported. While the 12 km × 12 km grid used here is the finest grid readily available for a national scale study, it still may not be fine enough to detect high air pollution hotspots in the immediate vicinity of sources, especially those that may coincide with areas that have high rates of background disease, and thus have potentially higher impacts at community scale.

Only the average emission estimates from FV using VIIRS data as shown in Table 1 were used in the air quality modeling and heath impact analyses. Furthermore, as discussed earlier, not all uncertainties (e.g., uncertainties in VIIRS FGV) were accounted for in the emission estimates. However, we expect impacts of such emission uncertainties on the air quality modeling results to be insignificant given the small magnitude of uncertainties (standard deviation of emissions <4%) and the small impact of flaring and venting (its contribution to critical pollutants <0.15%).

Table 2
Monetary Valuation of Health Impacts (in wFlare2 Scenario)

	Flaring health impact outcomes, based on pollutant type		
Health impact	Pollutant type	Number of cases (95% CI)	Monetary valuation ($1 million) (95% CI)
Premature Deaths	$PM_{2.5}$	360 (300–420)	3,700 (1,900–6,000)
	O_3	230 (120–470)	2,400 (720–6,800)
	NO_2	120 (61–180)	1,300 (380–2,700)
	All Three	710 (480–1,100)	7,300 (3,000–16,000)
Asthma Incidence	$PM_{2.5}$	140 (47–230)	8.2 (1.1–22)
	NO_2	47 (19–65)	2.8 (0.46–6.1)
	$PM_{2.5}$ and NO_2	190 (66–300)	11 (1.6–28)
Asthma Hospitalizations (Alhanti)	$PM_{2.5}$	1.3 (0.63–2.5)	0.023 (0.012–0.046)
	O_3	5.7 (3.2–8.1)	0.1 (0.059–0.15)
	NO_2	3.2 (2.5–4.5)	0.058 (0.046–0.081)
	All Three	10 (6.4–15)	0.18 (0.12–0.28)
Asthma Exacerbations (Alhanti)	$PM_{2.5}$	9,700 (4,900–19,000)	0.58 (0.11–1.9)
	O_3	43,000 (24,000–61,000)	2.5 (0.53–6)
	NO_2	21,000 (16,000–29,000)	1.2 (0.36–2.8)
	All Three	73,000 (46,000–110,000)	4.3 (0.99–11)
Asthma ED Visits (Alhanti)	$PM_{2.5}$	13 (6.3–25)	0.006 (0.003–0.012)
	O_3	54 (31–77)	0.024 (0.013–0.036)
	NO2	25 (20–36)	0.011 (0.009–0.017)
	All Three	92 (58–140)	0.042 (0.025–0.065)
Respiratory Hospitalizations	$PM_{2.5}$	19 (9.8–28)	0.57 (0.29–0.84)
	O_3	110 (40–180)	3.4 (1.2–5.5)
	$PM_{2.5}$ and Ozone	130 (50–210)	3.9 (1.5–6.4)
Heart Attacks	$PM_{2.5}$	16 (9.7–23)	1.1 (0.68–1.6)
	NO_2	6.9 (3.7–10)	0.48 (0.26–0.7)
	$PM_{2.5}$ and NO_2	23 (13–33)	1.6 (0.94–2.3)
Total			7,400 (3,000–16,000)

Although VIIRS-based emission estimates from FV in this study are shown to be higher than estimates in NEI 2017, neither estimate was further evaluated for its accuracy given the absence of large scale (e.g., county-level or O&G basin-wide) measurements of emissions from FV facilities. VIIRS's observation is considered as state-of-the-art method for detecting flare volumes and used in other recent studies (Chen et al., 2022; Dix et al., 2019, 2022; Francoeur et al., 2021; Zhang et al., 2015, 2021), offering better quantification of FGV than the FGV used in the NEI estimates which were based on underreported data from O&G facilities (BBC, 2022; DOE, 2019). However, multiple assumptions in heating values and emission factors are applied to this VIIRS's FGV, as discussed elsewhere in this manuscript, which lead to potential uncertainties in these emission estimates. While the overall modeling framework and methods used in our study are robust, well established and used in multiple prior health assessment studies, uncertainties in these emission estimates along with those from air quality models and health incidence input data sets further impact potential accuracy in our reported health incidence estimates from flaring and venting.

While the health impact modeling uses the best background health data available, some outcomes only have data at state or national resolution—missing potential hotspots for diseases, most notably asthma. Additionally, since the health modeling framework exclusively captures health impacts due to exposure to the three pollutants ozone, $PM_{2.5}$, and NO_2, this model is unlikely to fully capture many of the complex, multifactorial impacts occurring in communities hosting O&G production. These health outcomes include but are not limited

10.1029/2023GH000938

to adverse birth outcomes (Willis et al., 2022), asthma (Willis et al., 2018), and childhood leukemia (Clark et al., 2022).

The environmental justice analysis that we conducted was not comprehensive of all Justice40 Initiative indicators (Council on Environmental Quality, 2022) that were available. Future research could consider including other populations at risk of environmental exposures as defined by CJEST (Council on Environmental Quality, 2022). Furthermore, the U.S. Census Bureau American Community Survey (ACA) data underreports the true number of Native peoples living in the U.S. (Smithsonian, 2023), and the undercounting and misclassification of Native peoples in health databases (Jim et al., 2014; Stehr-Green et al., 2002) along with existing cultural, structural, and social barriers to health care (USCCR, 2004) contribute to the true representation of Native persons and their health status (Adakai et al., 2018). Having access to the true number of Native peoples and fairly represented mortality and asthma outcomes could alter our health impact calculations.

Despite these limitations, this study still produces a robust estimate of health impacts of flaring by using the best data available for emissions from flaring from two different sources. This study also uses a novel health impact assessment framework that includes health impacts of direct NO_2 exposure, and health outcomes not regularly included in air pollution health impact assessments, most notably birth and children's health outcomes.

4. Conclusions

Combining satellite-based observation of flare activities in O&G activities and a new set of emission factors resulted in higher emissions from FV in the U.S. than what was reported in the EPA's NEI. Impacts of FV on air quality are most noticeable and significant within FV-major areas and their immediate downwind regions, even though domain-wide averages are relatively small compared to the overall O&G impacts. However, the FV sector still contributes up to about $7.4B (about 10%) of the total burden of health risk from O&G, and thus highlighting the potential need to focus on them for protecting public health. Of the total 710 premature deaths estimated from FV, 360 are attributed to $PM_{2.5}$, 230 to O_3, and 120 to NO_2. This finding signifies that while most health impact studies so far have been focused on $PM_{2.5}$, health impact from O_3 and NO_2 should not be overlooked. Findings from this study suggest controlling emissions from flaring and venting from O&G production, besides being cost effective and profitable to the operators, additionally provides an opportunity for yielding significant public health benefits.

Conflict of Interest

The authors declare no conflicts of interest relevant to this study.

Data Availability Statement

Estimates of flared gas volume from the Visible Infrared Imaging Radiometer Suite—VIIRS for 2019 and other years are publicly available at EOG (2023). Monthly allocation of annual flare gas volume developed based on monthly vented and flared gas volume from U.S. EIA, publicly available at EIA (2023). National emissions inventories (NEI) data for 2016 and 2017 were downloaded from U.S. EPA Emission Modeling Platforms, publicly available at EPA (2023b). Flare stack parameters were estimated with reanalysis II wind data from NOAA Physical Sciences Laboratory, publicly available at NOAA (2023). Baseline health and economic data were extracted from U.S. EPA BenMAP model which is publicly available at EPA (2023a). Mortality and population counts for individual counties for the entire U.S. for adults ≥25 years and infants <1 year old were obtained from Centers for Disease Control and Prevention Wide-ranging ONline Data for Epidemiologic Research—CDC WONDER, available through request at CDC (2023a); user's agreement to data use restrictions is required. National trends in healthcare utilization, access, charges, quality, and outcomes were obtained from Healthcare Cost and Utilization Project (HCUP), publicly available at AHRQ (2022). Asthma exacerbations were evaluated with asthma prevalence data from Center for Disease Control and Prevention; publicly available at CDC (2018) and CDC (2023b). Environmental justice analysis was performed with data from the Climate and Economic Justice Screen Tool—CJEST, publicly available at CEQ (2023). Emission data was processed using the Sparse Matrix Operator Kernel Emissions—SMOKE version 4.8, publicly available at Baek and Seppanen (2020). Air quality simulations were performed using the Community Multiscale Air Quality—CMAQ model version 5.2.1, publicly available at EPA (2018). Source code of the BenMAPR is publicly available at jjbuonocore (2023).

Acknowledgments

This work was financially supported by grants from the Environmental Defense Fund and Global Methane Hub under Grant 016010-2022-01-01. We acknowledge Alison Eyth and Jeffrey Vukovich of the U.S. EPA for providing emissions inventories from the NEI and for various helpful discussions, and to all air quality scientists across multiple state, local, tribal, and regional agencies, and U. S. EPA and Federal Land Management agencies who were involved in the development of the national inventories. We also acknowledge the U.S. EPA for providing meteorological inputs from WRF and outputs from the CMAQ hemispherical scale simulations for extracting initial and boundary conditions used in this study.

References

Adakai, M., Sandoval-Rosario, M., Xu, F., Aseret-Manygoats, T., Allison, M., Greenlund, K. J., & Barbour, K. E. (2018). Health disparities among American Indians/Alaska natives - Arizona, 2017. *MMWR. Morbidity and Mortality Weekly Report*, *67*(47), 1314–1318. https://doi.org/10.15585/mmwr.mm6747a4

Ahmadov, R., McKeen, S., Trainer, M., Banta, R., Brewer, A., Brown, S., et al. (2015). Understanding high wintertime ozone pollution events in an oil- and natural gas-producing region of the western US. *Atmospheric Chemistry and Physics*, *15*(1), 411–429. https://doi.org/10.5194/acp-15-411-2015

AHRQ. (2022). Healthcare cost & utilization project (HCUP) user support databases [Dataset]. AHRQ. Retrieved from https://hcup-us.ahrq.gov/databases.jsp

Allen, D. T., Smith, D., Torres, V. M., & Saldaña, F. C. (2016). Carbon dioxide, methane and black carbon emissions from upstream oil and gas flaring in the United States. *Current Opinion in Chemical Engineering*, *13*, 119–123. https://doi.org/10.1016/j.coche.2016.08.014

Anejionu, O. C. D., Whyatt, J. D., Blackburn, G. A., & Price, C. S. (2015). Contributions of gas flaring to a global air pollution hotspot: Spatial and temporal variations, impacts and alleviation. *Atmospheric Environment*, *118*, 184–193. https://doi.org/10.1016/j.atmosenv.2015.08.006

Ansari, A. S., & Pandis, S. N. (1998). Response of inorganic PM to precursor concentrations. *Environmental Science & Technology*, *32*(18), 2706–2714. https://doi.org/10.1021/es971130j

Arter, C. A., Buonocore, J. J., Moniruzzaman, C., Yang, D., Huang, J., & Arunachalam, S. (2022). Air quality and health-related impacts of traditional and alternate jet fuels from airport aircraft operations in the. *U.S. Environment International*, *158*, 106958. https://doi.org/10.1016/j.envint.2021.106958

Baek, B. H., & Seppanen, C. (2020). CEMPD/SMOKE: SMOKE v4.8 public release (October 2020) (SMOKEv48_Oct2020) [Software]. Zenodo. https://doi.org/10.5281/zenodo.4088945

BBC. (2022). *Revealed: Huge gas flaring emissions never reported*. BBC News.

Blundell, W., & Kokoza, A. (2022). Natural gas flaring, respiratory health, and distributional effects. *Journal of Public Economics*, *208*, 104601. https://doi.org/10.1016/j.jpubeco.2022.104601

Buonocore, J. J., Reka, S., Yang, D., Chang, C., Roy, A., Thompson, T., et al. (2023). Air pollution and health impacts of oil & gas production in the United States. *Environmental Research: Health*, *1*(2), 021006. https://doi.org/10.1088/2752-5309/acc886

Byun, D., & Schere, K. L. (2006). Review of the governing equations, computational algorithms, and other components of the models-3 community multiscale air quality (CMAQ) modeling system. *Applied Mechanics Reviews*, *59*(2), 51–77. https://doi.org/10.1115/1.2128636

Caulton, D. R., Shepson, P. B., Cambaliza, M. O. L., McCabe, D., Baum, E., & Stirm, B. H. (2014). Methane destruction efficiency of natural gas flares associated with shale formation wells. *Environmental Science & Technology*, *48*(16), 9548–9554. https://doi.org/10.1021/es500511w

CDC. (2018). Asthma - Table 4-1 current asthma prevalence percents by age, 2017 national health interview survey (NHIS) data [Dataset]. Centers for Disease Control and Prevention (CDC). Retrieved from https://www.cdc.gov/asthma/nhis/2017/table4-1.htm

CDC. (2023a). Compressed mortality, 1999-2016 request [Dataset]. Centers for Disease Control and Prevention (CDC). Retrieved from https://wonder.cdc.gov/cmf-icd10.html

CDC. (2023b). National environmental public health tracking network data explorer [Dataset]. Centers for Disease Control and Prevention (CDC). Retrieved from https://ephtracking.cdc.gov/DataExplorer/

CEQ. (2022). CJEST data download [Dataset]. Council on Environmental Quality (CEQ). Retrieved from https://screeningtool.geoplatform.gov/en/#3/33.47/-97.5

Chen, C., McCabe, D. C., Fleischman, L. E., & Cohan, D. S. (2022). Black carbon emissions and associated health impacts of gas flaring in the United States. *Atmosphere*, *13*(3), 385. https://doi.org/10.3390/atmos13030385

Clark, C. J., Johnson, N. P., Soriano, M., Warren, J. L., Sorrentino, K. M., Kadan-Lottick, N. S., et al. (2022). Unconventional oil and gas development exposure and risk of childhood acute lymphoblastic Leukemia: A case-control study in Pennsylvania, 2009-2017. *Environmental Health Perspectives*, *130*(8), 87001. https://doi.org/10.1289/EHP11092

Council on Environmental Quality. (2022). Climate and economic justice screen tool (CJEST). Retrieved from https://screeningtool.geoplatform.gov/en/downloads

Cushing, L. J., Chau, K., Franklin, M., & Johnston, J. E. (2021). Up in smoke: Characterizing the population exposed to flaring from unconventional oil and gas development in the contiguous US. *Environmental Research Letters*, *16*(3), 034032. https://doi.org/10.1088/1748-9326/abd3d4

Cushing, L. J., Vavra-Musser, K., Chau, K., Franklin, M., & Johnston, J. E. (2020). Flaring from unconventional oil and gas development and birth outcomes in the eagle ford shale in South Texas. *Environmental Health Perspectives*, *128*(7), 77003. https://doi.org/10.1289/EHP6394

Dix, B., Bruin, J., Roosenbrand, E., Vlemmix, T., Francoeur, C., Gorchov-Negron, A., et al. (2019). Nitrogen oxide emissions from U.S. oil and gas production: Recent trends and source attribution. *Geophysical Research Letters*. https://doi.org/10.1029/2019GL085866

Dix, B., Francoeur, C., Li, M., Serrano-Calvo, R., Levelt, P. F., Veefkind, J. P., et al. (2022). Quantifying NO emissions from U.S. oil and gas production regions using TROPOMI NO_2. *ACS Earth and Space Chemistry*, *6*(2), 403–414. https://doi.org/10.1021/acsearthspacechem.1c00387

DOE. (2019). Natural gas flaring and venting: State and federal regulatory overview, tends, and impacts.

Edwards, P. M., Brown, S. S., Roberts, J. M., Ahmadov, R., Banta, R. M., de Gouw, J., et al. (2014). High winter ozone pollution from carbonyl photolysis in an oil and gas basin. *Nature*, *514*(7522), 351–354. https://doi.org/10.1038/nature13767

Edwards, P. M., Young, C. J., Aikin, K., de Gouw, J., Dubé, W. P., Geiger, F., et al. (2013). Ozone photochemistry in an oil and natural gas extraction region during winter: Simulations of a snow-free season in the Uintah Basin, Utah. *Atmospheric Chemistry and Physics*, *13*(17), 8955–8971. https://doi.org/10.5194/acp-13-8955-2013

EIA. (2023). Natural gas vented and flared summary [Dataset]. EIA. Retrieved from https://www.eia.gov/dnav/ng/NG_SUM_LSUM_A_EPG0_VGV_MMCF_A.htm

Elvidge, C., Zhizhin, M., Baugh, K., Hsu, F.-C., & Ghosh, T. (2015). Methods for global survey of natural gas flaring from visible infrared imaging radiometer suite data. *Energies*, *9*(1), 14. https://doi.org/10.3390/en9010014

Elvidge, C., Zhizhin, M., Hsu, F.-C., & Baugh, K. (2013). VIIRS nightfire: Satellite pyrometry at night. *Remote Sensing*, *5*(9), 4423–4449. https://doi.org/10.3390/rs5094423

Elvidge, C. D., Bazilian, M. D., Zhizhin, M., Ghosh, T., Baugh, K., & Hsu, F.-C. (2018). The potential role of natural gas flaring in meeting greenhouse gas mitigation targets. *Energy Strategy Reviews*, *20*, 156–162. https://doi.org/10.1016/j.esr.2017.12.012

EOG. (2023). Global gas flaring observation from space [Dataset]. Earth Observation Group (EOG). Retrieved from https://eogdata.mines.edu/products/vnf/global_gas_flare.html

EPA. (2018). Community multiscale air quality (CMAQ) model version 5.2.1 [Software]. U.S. Environment Protection Agency (EPA) Office of Research and Development. Zenodo. https://doi.org/10.5281/zenodo.1212601

EPA. (2023a). Benefits mapping and analysis program (BenMAP) downloads [Dataset]. U.S. Environment Protection Agency (EPA). Retrieved from https://www.epa.gov/benmap/benmap-downloads

EPA. (2023b). Emissions modeling platforms [Dataset]. U.S. Environment Protection Agency (EPA). Retrieved from https://www.epa.gov/air-emissions-modeling/emissions-modeling-platforms

Fawole, O. G., Cai, X. M., & MacKenzie, A. R. (2016). Gas flaring and resultant air pollution: A review focusing on black carbon. *Environmental Pollution*, *216*, 182–197. https://doi.org/10.1016/j.envpol.2016.05.075

Francoeur, C. B., McDonald, B. C., Gilman, J. B., Zarzana, K. J., Dix, B., Brown, S. S., et al. (2021). Quantifying methane and ozone precursor emissions from oil and gas production regions across the contiguous US. *Environmental Science & Technology*, *55*(13), 9129–9139. https://doi.org/10.1021/acs.est.0c07352

GGFR. (2023). Global gas flaring reduction partnership (GGFR). Retrieved from https://www.worldbank.org/en/programs/gasflaringreduction/gas-flaring-explained

Gorchov Negron, A. M., McDonald, B. C., McKeen, S. A., Peischl, J., Ahmadov, R., de Gouw, J. A., et al. (2018). Development of a fuel-based oil and gas inventory of nitrogen oxides emissions. *Environmental Science & Technology*, *52*(17), 10175–10185. https://doi.org/10.1021/acs.est.8b02245

Gvakharia, A., Kort, E. A., Brandt, A., Peischl, J., Ryerson, T. B., Schwarz, J. P., et al. (2017). Methane, black carbon, and ethane emissions from natural gas flares in the Bakken Shale, North Dakota. *Environmental Science & Technology*, *51*(9), 5317–5325. https://doi.org/10.1021/acs.est.6b05183

Jim, M. A., Arias, E., Seneca, D. S., Hoopes, M. J., Jim, C. C., Johnson, N. J., & Wiggins, C. L. (2014). Racial misclassification of American Indians and Alaska natives by Indian health service contract health service delivery area. *American Journal of Public Health*, *104*(3), S295–S302. https://doi.org/10.2105/AJPH.2014.301933

jjbuonocore. (2023). jjbuonocore/BenMAPR: BenMAPR for O&G (version v1) [Software]. Zenodo. https://doi.org/10.5281/zenodo.8306380

Knighton, W. B., Herndon, S. C., Franklin, J. F., Wood, E. C., Wormhoudt, J., Brooks, W., et al. (2012). Direct measurement of volatile organic compound emissions from industrial flares using real-time online techniques: Proton transfer reaction mass spectrometry and tunable infrared laser differential absorption spectroscopy. *Industrial & Engineering Chemistry Research*, *51*(39), 12674–12684. https://doi.org/10.1021/ie202695v

Lyon, D. R., Hmiel, B., Gautam, R., Omara, M., Roberts, K. A., Barkley, Z. R., et al. (2021). Concurrent variation in oil and gas methane emissions and oil price during the COVID-19 pandemic. *Atmospheric Chemistry and Physics*, *21*(9), 6605–6626. https://doi.org/10.5194/acp-21-6605-2021

McDuffie, E. E., Edwards, P. M., Gilman, J. B., Lerner, B. M., Dubé, W. P., Trainer, M., et al. (2016). Influence of oil and gas emissions on summertime ozone in the Colorado Northern Front Range. *Journal of Geophysical Research: Atmospheres*, *121*(14), 8712–8729. https://doi.org/10.1002/2016JD025265

Motte, J., Alvarenga, R. A. F., Thybaut, J. W., & Dewulf, J. (2021). Quantification of the global and regional impacts of gas flaring on human health via spatial differentiation. *Environmental Pollution*, *291*, 118213. https://doi.org/10.1016/j.envpol.2021.118213

NOAA. (2023). NCEP/DOE reanalysis II [Dataset]. National Oceanic and Atmospheric Administration Physical Sciences Laboratory (NOAA). Retrieved from https://psl.noaa.gov/data/gridded/data.ncep.reanalysis2.html

Olaguer, E. P. (2012a). Near-source air quality impacts of large olefin flares. *Journal of the Air & Waste Management Association (1995)*, *62*(8), 978–988. https://doi.org/10.1080/10962247.2012.693054

Olaguer, E. P. (2012b). The potential near-source ozone impacts of upstream oil and gas industry emissions. *Journal of the Air & Waste Management Association (1995)*, *62*(8), 966–977. https://doi.org/10.1080/10962247.2012.688923

Park, R. J., Jacob, D. J., Field, B. D., Yantosca, R. M., & Chin, M. (2004). Natural and transboundary pollution influences on sulfate-nitrate-ammonium aerosols in the United States: Implications for policy. *Journal of Geophysical Research*, *109*(D15), D15204. https://doi.org/10.1029/2003JD004473

Plant, G., Kort, E. A., Brandt, A. R., Chen, Y., Fordice, G., Gorchov Negron, A. M., et al. (2022). Inefficient and unlit natural gas flares both emit large quantities of methane. *Science*, *377*(6614), 1566–1571. https://doi.org/10.1126/science.abq0385

Pohl, J. H., Tichenor, B. A., Lee, J., & Payne, R. (1986). Combustion efficiency of flares. *Combustion Science and Technology*, *50*(4–6), 217–231. https://doi.org/10.1080/00102208608923934

Reuters (2022). Never dark for families under the red glow of Mexico's gas flares. Retrieved from https://www.reuters.com/investigates/special-report/mexico-pemex-flaring/

Rystad Energy. (2022). *Cost of flaring abatement - Final report* (p. 112). Prepared by Rystad Energy for Environmental Defense Fund.

Sacks, J. D., Lloyd, J. M., Zhu, Y., Anderton, J., Jang, C. J., Hubbell, B., & Fann, N. (2018). The environmental benefits mapping and analysis program – Community edition (BenMAP–CE): A tool to estimate the health and economic benefits of reducing air pollution. *Environmental Modelling & Software*, *104*, 118–129. https://doi.org/10.1016/j.envsoft.2018.02.009

Schade, G. W. (2021). Standardized reporting needed to improve accuracy of flaring data. *Energies*, *14*(20), 6575. https://doi.org/10.3390/en14206575

Schwarz, J. P., Holloway, J. S., Katich, J. M., McKeen, S., Kort, E. A., Smith, M. L., et al. (2015). Black carbon emissions from the bakken oil and gas development region. *Environmental Science and Technology Letters*, *2*(10), 281–285. https://doi.org/10.1021/acs.estlett.5b00225

Shaw, J. T., Foulds, A., Wilde, S., Barker, P., Squires, F., Lee, J., et al. (2022). Flaring efficiencies and NO_x emission ratios measured for offshore oil and gas facilities in the North Sea. https://doi.org/10.5194/acp-2022-679

Skamarock, W., Klemp, J., Dudhia, J., Gill, D., Barker, D., Wang, W., et al. (2008). *A description of the advanced research WRF version 3*. UCAR/NCAR. https://doi.org/10.5065/d68s4mvh

Smithosian (2023). Frequently asked questions | Native knowledge 360° - Interactive teaching resources. Retrieved from https://americanindian.si.edu/nk360/faq/did-you-know#

Soltanieh, M., Zohrabian, A., Gholipour, M. J., & Kalnay, E. (2016). A review of global gas flaring and venting and impact on the environment: Case study of Iran. *International Journal of Greenhouse Gas Control*, *49*, 488–509. https://doi.org/10.1016/j.ijggc.2016.02.010

Stehr-Green, P., Bettles, J., & Robertson, L. D. (2002). Effect of racial/ethnic misclassification of American Indians and Alaskan Natives on Washington State death certificates, 1989-1997. *American Journal of Public Health*, *92*(3), 443–444. https://doi.org/10.2105/ajph.92.3.443

TCEQ. (2004). Technical basis for flare parameters. Retrieved from https://www.tceq.texas.gov/assets/public/permitting/air/memos/flareparameters.pdf

Tyner, D. R., & Johnson, M. R. (2021). Where the methane is-insights from novel airborne LiDAR measurements combined with ground survey data. *Environmental Science & Technology*, *55*(14), 9773–9783. https://doi.org/10.1021/acs.est.1c01572

UDEQ. (2022). 2020 statewide oil & gas emissions inventory. Retrieved from https://deq.utah.gov/air-quality/statewide-oil-gas-emissions-inventory

Umukoro, G. E., & Ismail, O. S. (2017). Modelling emissions from natural gas flaring. *Journal of King Saud University - Engineering Sciences*, *29*(2), 178–182. https://doi.org/10.1016/j.jksues.2015.08.001

USCCR. (2004). *Broken promises: Evaluating the native American health care system*. U.S. Commission on Civil Rights (USCCR). Retrieved from https://www.usccr.gov/files/pubs/docs/nabroken.pdf

Weyant, C. L., Shepson, P. B., Subramanian, R., Cambaliza, M. O. L., Heimburger, A., McCabe, D., et al. (2016). Black carbon emissions from associated natural gas flaring. *Environmental Science & Technology*, *50*(4), 2075–2081. https://doi.org/10.1021/acs.est.5b04712

Willis, M. D., Hill, E. L., Kile, M. L., Carozza, S., & Hystad, P. (2022). Associations between residential proximity to oil and gas extraction and hypertensive conditions during pregnancy: A difference-in-differences analysis in Texas, 1996-2009. *International Journal of Epidemiology*, *51*(2), 525–536. https://doi.org/10.1093/ije/dyab246

Willis, M. D., Jusko, T. A., Halterman, J. S., & Hill, E. L. (2018). Unconventional natural gas development and pediatric asthma hospitalizations in Pennsylvania. *Environmental Research*, *166*, 402–408. https://doi.org/10.1016/j.envres.2018.06.022

Willyard, K. A., & Schade, G. W. (2019). Flaring in two Texas shale areas: Comparison of bottom-up with top-down volume estimates for 2012 to 2015. *The Science of the Total Environment*, *691*, 243–251. https://doi.org/10.1016/j.scitotenv.2019.06.465

Womack, C. C., McDuffie, E. E., Edwards, P. M., Bares, R., Gouw, J. A., Docherty, K. S., et al. (2019). An odd oxygen framework for wintertime ammonium nitrate aerosol pollution in urban areas: NOx and VOC control as mitigation strategies. *Geophysical Research Letters*, *46*(9), 4971–4979. https://doi.org/10.1029/2019GL082028

World Bank. (2022). 2022 global gas flaring tracker report. Retrieved from https://www.worldbank.org/en/topic/extractiveindustries/publication/2022-global-gas-flaring-tracker-report

Wyat Appel, K., Napelenok, S., Hogrefe, C., Pouliot, G., Foley, K. M., Roselle, S. J., et al. (2018). Overview and evaluation of the community multiscale air quality (CMAQ) modeling system version 5.2. In C. Mensink & G. Kallos (Eds.), *Air pollution modeling and its application XXV* (pp. 69–73). Springer International Publishing.

Zhang, X., Scheving, B., Shoghli, B., Zygarlicke, C., & Wocken, C. (2015). Quantifying gas flaring CH_4 consumption using VIIRS. *Remote Sensing*, *7*(8), 9529–9541. https://doi.org/10.3390/rs70809529

Zhang, Z., Sherwin, E. D., & Brandt, A. R. (2021). Estimating global oilfield-specific flaring with uncertainty using a detailed geographic database of oil and gas fields. *Environmental Research Letters*, *16*(12), 124039. https://doi.org/10.1088/1748-9326/ac3956

Zhizhin, M., Matveev, A., Ghosh, T., Hsu, F.-C., Howells, M., & Elvidge, C. (2021). Measuring gas flaring in Russia with multispectral VIIRS nightfire. *Remote Sensing*, *13*(16), 3078. https://doi.org/10.3390/rs13163078

References From the Supporting Information

Alhanti, B. A., Chang, H. H., Winquist, A., Mulholland, J. A., Darrow, L. A., & Sarnat, S. E. (2016). Ambient air pollution and emergency department visits for asthma: A multi-city assessment of effect modification by age. *Journal of Exposure Science and Environmental Epidemiology*, *26*(2), 180–188. https://doi.org/10.1038/jes.2015.57

Appel, K. W., Bash, J. O., Fahey, K. M., Foley, K. M., Gilliam, R. C., Hogrefe, C., et al. (2021). The community multiscale air quality (CMAQ) model versions 5.3 and 5.3.1: System updates and evaluation. *Geoscientific Model Development*, *14*(5), 2867–2897. https://doi.org/10.5194/gmd-14-2867-2021

Appel, K. W., Napelenok, S. L., Foley, K. M., Pye, H. O. T., Hogrefe, C., Luecken, D. J., et al. (2017). Description and evaluation of the community multiscale air quality (CMAQ) modeling system version 5.1. *Geoscientific Model Development*, *10*(4), 1703–1732. https://doi.org/10.5194/gmd-10-1703-2017

API. (2014). *API Standard 521 (No. C52106, 6th ed.)* (p. 248). American Petroleum Institute (API).

Becerra, T. A., Wilhelm, M., Olsen, J., Cockburn, M., & Ritz, B. (2013). Ambient air pollution and autism in Los Angeles county, California. *Environmental Health Perspectives*, *121*(3), 380–386. https://doi.org/10.1289/ehp.1205827

EPA. (2023c). AP-42: Compilation of air emissions factors. Retrieved from https://www.epa.gov/air-emissions-factors-and-quantification/ap-42-compilation-air-emissions-factors

EPA. (2023d). EPA proposes to strengthen air quality standards to protect the public from harmful effects of soot. Retrieved from https://www.epa.gov/newsreleases/epa-proposes-strengthen-air-quality-standards-protect-public-harmful-effects-soot

ERG. (2022). *2020 nonpoint oil and gas emission estimation tool version 1.3*. Eastern Research Group, Inc. (ERG).

Faustini, A., Rapp, R., & Forastiere, F. (2014). Nitrogen dioxide and mortality: Review and meta-analysis of long-term studies. *European Respiratory Journal*, *44*(3), 744–753. https://doi.org/10.1183/09031936.00114713

Flores, N. M., McBrien, H., Do, V., Kiang, M. V., Schlegelmilch, J., & Casey, J. A. (2023). The 2021 Texas power crisis: Distribution, duration, and disparities. *Journal of Exposure Science and Environmental Epidemiology*, *33*(1), 21–31. https://doi.org/10.1038/s41370-022-00462-5

Ji, M., Cohan, D. S., & Bell, M. L. (2011). Meta-analysis of the association between short-term exposure to ambient ozone and respiratory hospital admissions. *Environmental Research Letters*, *6*(2), 024006. https://doi.org/10.1088/1748-9326/6/2/024006

Khreis, H., Kelly, C., Tate, J., Parslow, R., Lucas, K., & Nieuwenhuijsen, M. (2017). Exposure to traffic-related air pollution and risk of development of childhood asthma: A systematic review and meta-analysis. *Environment International*, *100*, 1–31. https://doi.org/10.1016/j.envint.2016.11.012

Levy, J. I., Diez, D., Dou, Y., Barr, C. D., & Dominici, F. (2012). A meta-analysis and multisite time-series analysis of the differential toxicity of major fine particulate matter constituents. *American Journal of Epidemiology*, *175*(11), 1091–1099. https://doi.org/10.1093/aje/kwr457

Mustafic, H., Jabre, P., Caussin, C., Murad, M. H., Escolano, S., Tafflet, M., et al. (2012). Main air pollutants and myocardial infarction: A systematic review and meta-analysis. *The Journal of the American Medical Association*, *307*(7), 713–721. https://doi.org/10.1001/jama.2012.126

Nurmagambetov, T., Kuwahara, R., & Garbe, P. (2018). The economic burden of asthma in the United States, 2008-2013. *Annals of the American Thoracic Society*, *15*(3), 348–356. https://doi.org/10.1513/AnnalsATS.201703-259OC

Ostro, B., Lipsett, M., Mann, J., Braxton-Owens, H., & White, M. (2001). Air pollution and exacerbation of asthma in African-American children in Los Angeles. *Epidemiology*, *12*(2), 200–208. https://doi.org/10.1097/00001648-200103000-00012

Orellano, P., Quaranta, N., Reynoso, J., Balbi, B., & Vasquez, J. (2017). Effect of outdoor air pollution on asthma exacerbations in children and adults: Systematic review and multilevel meta-analysis. *PLoS One*, *12*(3), e0174050. https://doi.org/10.1371/journal.pone.0174050

Russell, R. B., Green, N. S., Steiner, C. A., Meikle, S., Howse, J. L., Poschman, K., et al. (2007). Cost of hospitalization for preterm and low birth weight infants in the United States. *Pediatrics*, *120*(1), e1–e9. https://doi.org/10.1542/peds.2006-2386

SJVAPCD. (2022). Inventory & modeling resources. Retrieved from https://www.valleyair.org/busind/pto/Resources/resources_idx.htm

Sun, X., Luo, X., Zhao, C., Chung Ng, R. W., Lim, C. E. D., Zhang, B., & Liu, T. (2015). The association between fine particulate matter exposure during pregnancy and preterm birth: A meta-analysis. *BMC Pregnancy and Childbirth*, *15*(1), 300. https://doi.org/10.1186/s12884-015-0738-2

Sun, X., Luo, X., Zhao, C., Zhang, B., Tao, J., Yang, Z., et al. (2016). The associations between birth weight and exposure to fine particulate matter (PM2.5) and its chemical constituents during pregnancy: A meta-analysis. *Environmental Pollution*, *211*, 38–47. https://doi.org/10.1016/j.envpol.2015.12.022

Torres, V. M., Herndon, S., Wood, E., Al-Fadhli, F. M., & Allen, D. T. (2012). Emissions of nitrogen oxides from flares operating at low flow conditions. *Industrial & Engineering Chemistry Research*, *51*(39), 12600–12605. https://doi.org/10.1021/ie300179x

Turner, M. C., Jerrett, M., Pope, C. A., Krewski, D., Gapstur, S. M., Diver, W. R., et al. (2016). Long-term ozone exposure and mortality in a large prospective study. *American Journal of Respiratory and Critical Care Medicine*, *193*(10), 1134–1142. https://doi.org/10.1164/rccm.201508-1633OC

Winer, R. A., Qin, X., Harrington, T., Moorman, J., & Zahran, H. (2012). Asthma incidence among children and adults: Findings from the Behavioral Risk Factor Surveillance system asthma call-back survey--United States, 2006-2008. *Journal of Asthma*, *49*(1), 16–22. https://doi.org/10.3109/02770903.2011.637594

Vodonos, A., Awad, Y. A., & Schwartz, J. (2018). The concentration-response between long-term PM2.5 exposure and mortality; A meta-regression approach. *Environmental Research*, *166*, 677–689. https://doi.org/10.1016/j.envres.2018.06.021

Zanobetti, A., Franklin, M., Koutrakis, P., & Schwartz, J. (2009). Fine particulate air pollution and its components in association with cause-specific emergency admissions. *Environmental Health: A Global Access Science Source*, *8*(1), 58. https://doi.org/10.1186/1476-069X-8-58